

APPENDIX

Worldwide infrared and millimeter wave satellite performance

Paul Christopher*
PFC Associates

ABSTRACT

Infrared satellite communication system performance is estimated from Barbaliscia's worldwide millimeter wave attenuation maps. The attenuation maps are used to derive new results for total liquid water content in clouds, which in turn is used to estimate 10 micron and 1 micron attenuation. The liquid water content of severe cloud cover is found to be fatal for most laser satcom, but cloud cover at the 80 percentile level would allow attractive 10 micron satellite communication throughout most of the Rocky Mountain States and the state of Maine. Site diversity, with sites separated by 100 km, would allow the infrared system to approach normal satcom reliability standards.

Keywords: Infrared, millimeter wave, satellite communication, orbits, cloud water content, probability

1.0 BACKGROUND

The Jet Propulsion Laboratory and Kim have recognized that optical communication^{1,2} near one micron wavelength can offer significant broadband advantages for satellite to ground communication links. They recognized that optical advantages over conventional satellite frequencies at 12-14 GHz included small size, low cost, convenient signal processing, and freedom from government frequency regulations. The Ground-to-Orbit Laser Demonstration (GOLD) has been planned for a few selected ground stations such as Mt. Lemmon in Arizona and sites in California that have been chosen for low atmospheric loss. Only a few selected sites were chosen because cloud attenuation has been assumed to be fatal for any satellite laser communication system. This paper shows millimeter wave attenuation estimates and then derives new cloud water content as a function of probability. Cloud water content estimates are shown as maps over large areas of the earth. It then shows that infrared lasers near the 10 micron wavelength region would usually be successful in traversing clouds at interesting locations.

More than three decades ago³, Chu and Hogg attempted to compare optical communication with infrared communication at 10.6 microns for terrestrial communication. They found that 10 micron signals propagated much better through fog than did the optical communication. Fig. 1-1 indicates the kind of signal loss they anticipated over a wide range of frequencies. The upper curve indicates loss through 1 km of fog with 0.1 gm/m³ liquid water density, vs Frequency on the abscissa. Note that 10 microns corresponds to 30 THz and the 1 micron region corresponds to 300 THz. The fog comparison for this figure indicates about 60 dB and 200 dB loss, respectively, for the two frequencies.

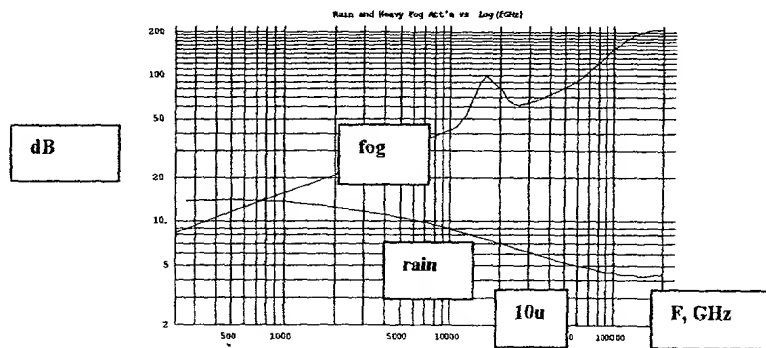


Fig. 1-1 Chu and Hogg's Fog(top) and Rain Attenuation(dB) v. Frequency
Note, 10u at 30THz and 1u at 300 THz

*312 Loudoun St., SW, Leesburg, VA 20175; phone 703-777-3239; pfchristop@aol.com

The Chu and Hogg insights lay in limbo during the development of satellite communication in the ensuing three decades. This was due to at least one reason, and probably a second. The total water content of clouds was not known, and the worst was naturally assumed as such high water content that neither optical (1 micron) nor infrared communication at 10 microns could be possible. This paper will use recent results in Italy^{4,5} and the US^{6,7,8} to derive new cloud water content estimates at specific probabilities, and the results will be plotted as maps of water content and attenuation over most of the earth. The infrared links will be shown to be unexpectedly promising in the Western US and in the Northeastern US, for much wider interest than the optical links. They would also retain most of the advantages of optical links.

2.0 WORLDWIDE CLOUD WATER CONTENT

The key work of Barbaliscia, Boumis, and Martellucci^{4,5} will allow us to derive and present worldwide estimates of cloud water content and implied signal absorption. Their 22.2 GHz absorption maps and their 49.5 GHz maps were chosen for 99% non-rainy conditions, or they may be thought of as a condition just prior to the commencement of rain. They were of interest^{6,7} for deriving a general attenuation function for the 10 to 100GHz region and the long attenuation equation was released on a floppy at the Ka conference in Cleveland⁷. The long function is too long to be included here (although the figures here include the long function) and Appendix A lists a shorter approximation. Fig. 2-1 shows an example of the derived zenith attenuation function(dB) at 30 GHz and LA, Rome and Rio are included for orientation on the map. Typical zenith attenuation at 30 GHz is less than 2 dB. When weighted by the cosecant of elevation angle for 3 GEO satellites, the attenuation function shows sharp attenuation cusps between the satellites (Fig. 2-2).

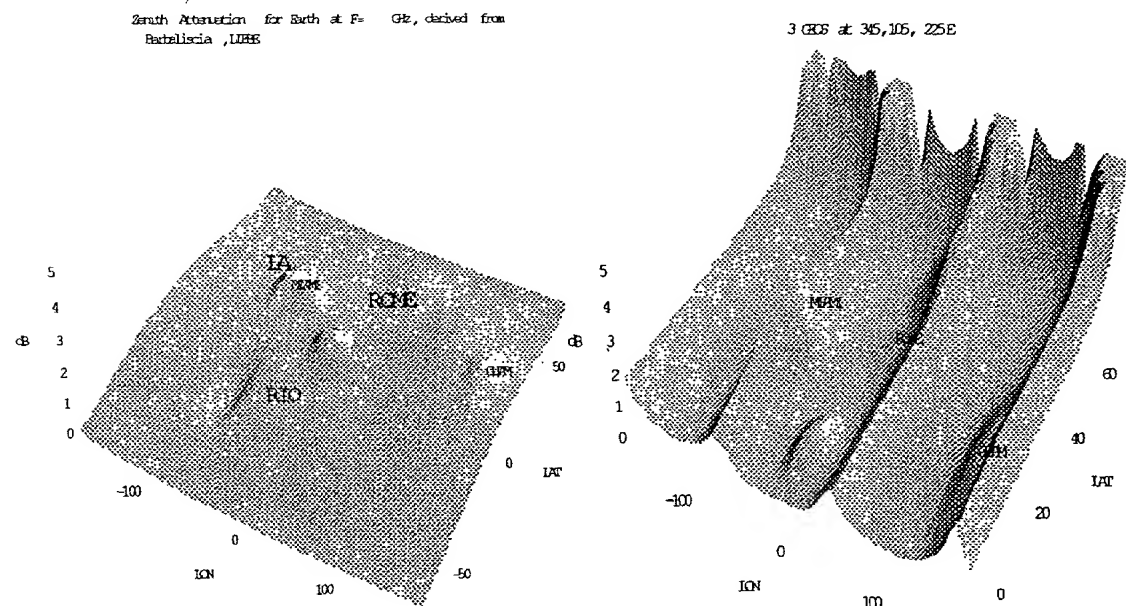


Fig. 2-1 Zenith Attenuation vs LON,LAT; 30GHz
(note LA, Rome, Rio) 99% nonrainy

Fig. 2-2 Attenuation for 3 GEOs
345E, 105E, 225E

Molniya satellites (Figs. 2-3 and 2-4) offer superior elevation angles and lower attenuation than GEOs. Fig. 2-5 gives the attenuation map for a combination of 3 Molniya plus 2 GEOs (total 5 satellites) for the 99% nonrainy condition at 30 GHz. Loss can also be seen as a function of frequency in Fig. 2-6 for three locations, with New York as the middle curve. For a fixed size and (nearly) fixed cost system, the increasing gain of a fixed aperture system may be shown as Net Loss (Fig. 2-7). Note that minimum Net

Loss at New York appears at 44 GHz and is nearly as low at 80 GHz. This appears as a pattern, and optimum frequency (Fig. 2-8) jumps sharply at latitudes north of New York City (40N).

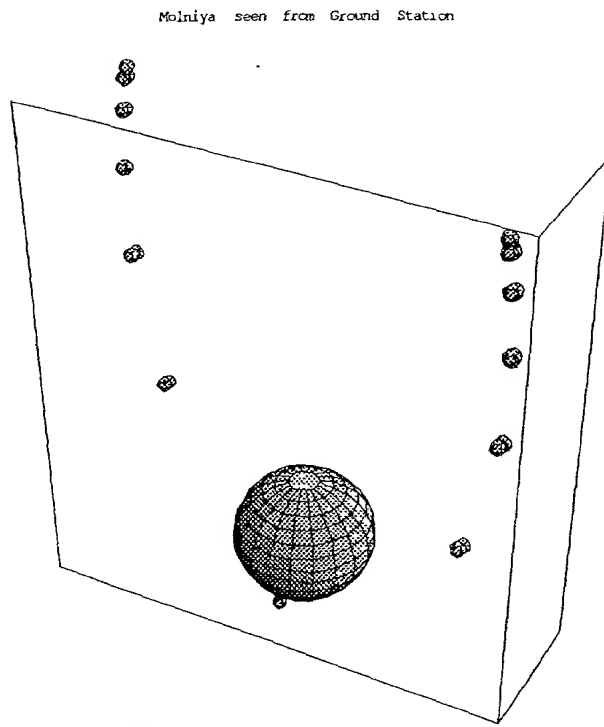


Fig. 2-3 Molniya (1 hour snapshots) as seen by Ground Station

The elevation probability density function (pdf) may be found as a function of Latitude (LAT) as:

MolniyaGEO pdf=

$$\frac{e^{-\frac{(5.22822 \times 10^{-6} \text{LAT}^4 - 0.000520006 \text{LAT}^3 + 0.00612491 \text{LAT}^2 + 0.165865 \text{LAT} + x - 47.0509)^2}{2 \left(0.000029238 \text{LAT}^4 - 0.00526509 \text{LAT}^3 + 0.270942 \text{LAT}^2 - 0.776901 \text{LAT} + 181.722 e^{-\frac{\text{LAT}^2}{900}} - 160.041 \right)^2}}}{\sqrt{2\pi}}$$

With x representing elevation angle in degrees.

$P(E, \text{Lat})$; 3 Molniya +2 Geo sats .

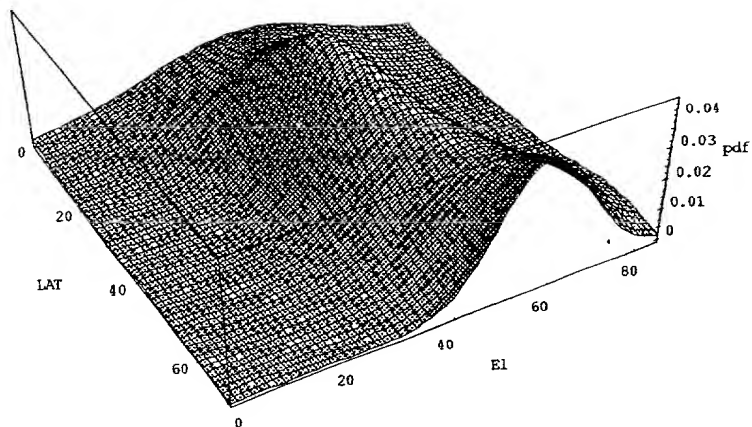


Fig 2-4 MolniyaGEO Elevation pdf vs Latitude

The elevation pdf can be used as an operator on the zenith attenuation to yield the MolniyaGEO loss at 30 GHz as Fig. 2-5.

MolniyaGEO Attenuation for N. Hemisphere at $F = 30$ GHz, by
Barcaliscia , LIFFE

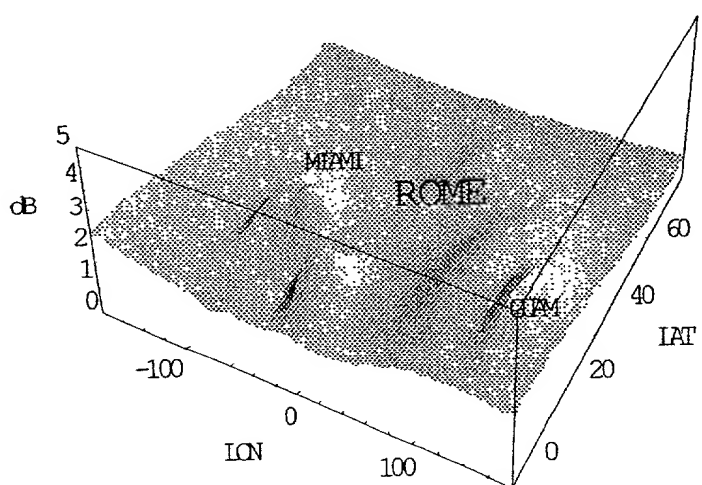


Fig. 2-5 30 GHz Attenuation for MolniyaGEO Constellation

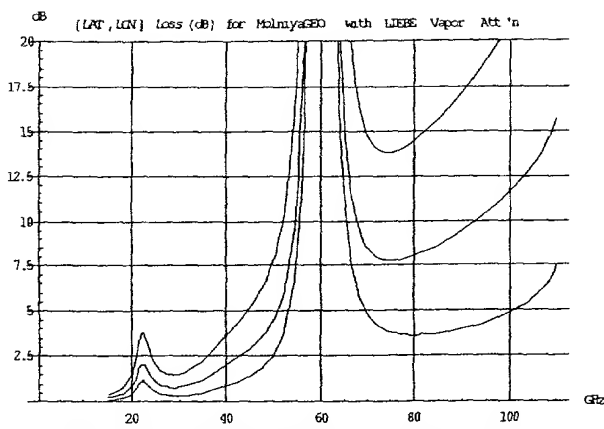


Fig. 2-6 MolniyaGEO Loss at Cuba, NY, Iceland vs Frequency (GHz)

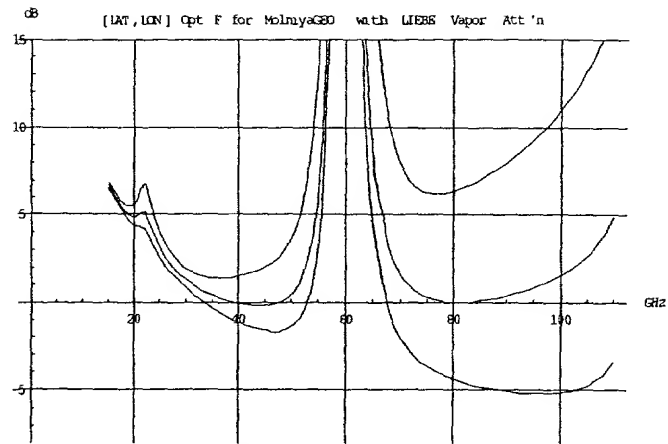


Fig. 2-7 Net Loss at Constant Aperture at Cuba, NY, Iceland, top to bottom

Trend of Optimum Frequency for MOIINYAEO v LON, LAT

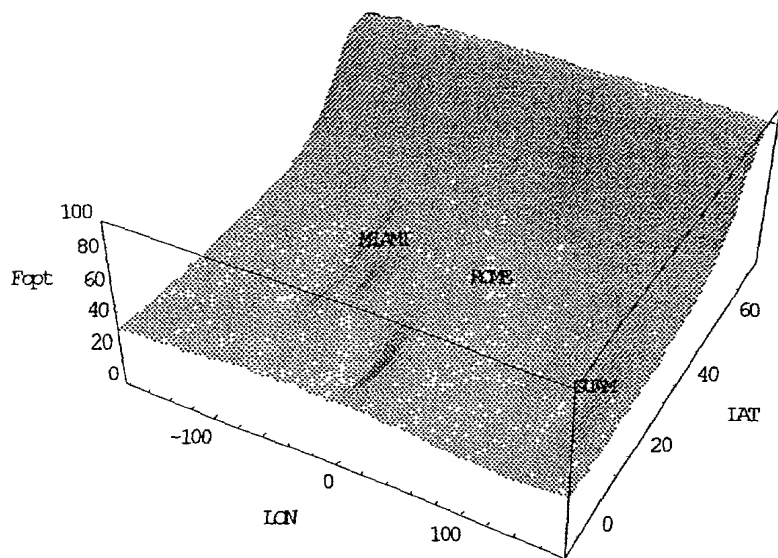


Fig. 2-8 Optimum Millimeter Wave Frequency vs LON,LAT
99% Nonrainy Attenuation

We note that optimum frequencies in the millimeter wave region appears at first glance to be a mirror image of the attenuation maps, with low optimum frequencies appearing (i.e., Miami) in regions of high attenuation. Also, attractive frequencies jump to the 90 GHz region at northern latitudes.

Infrared and optical frequencies are sharply affected by cloud attenuation. The methods used above for the millimeter wave attenuation can also be used to separate the effects of clouds and water vapor, and the net effect of cloud attenuation at 22.2 GHz can be found. This attenuation can be further interpreted, with the aid of Chu and Hogg (Fig. 1-1), as total water content in the clouds (Fig. 2-9). It is shown here with units of gm/m² as seen by a ray passing perpendicularly through the clouds, from a ground antenna pointed at zenith. Fig. 2-9 is believed to be a new result.

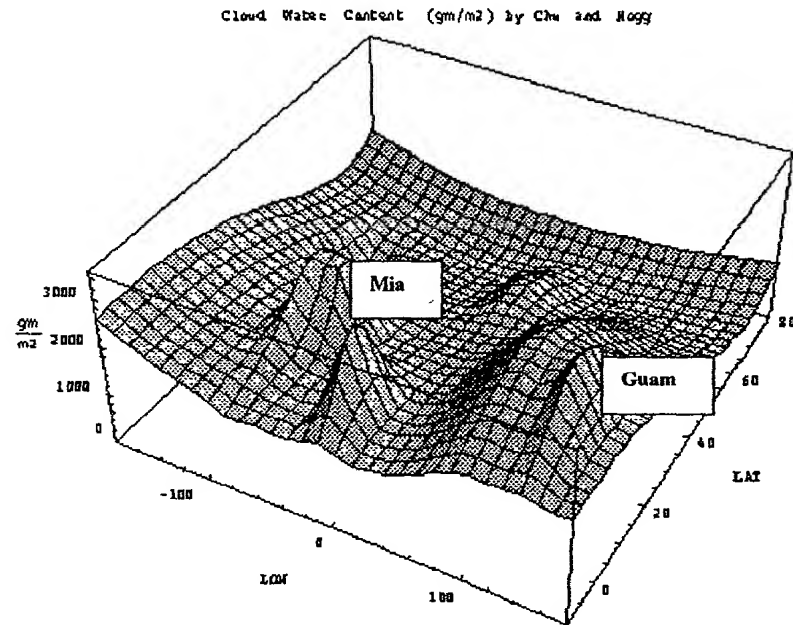
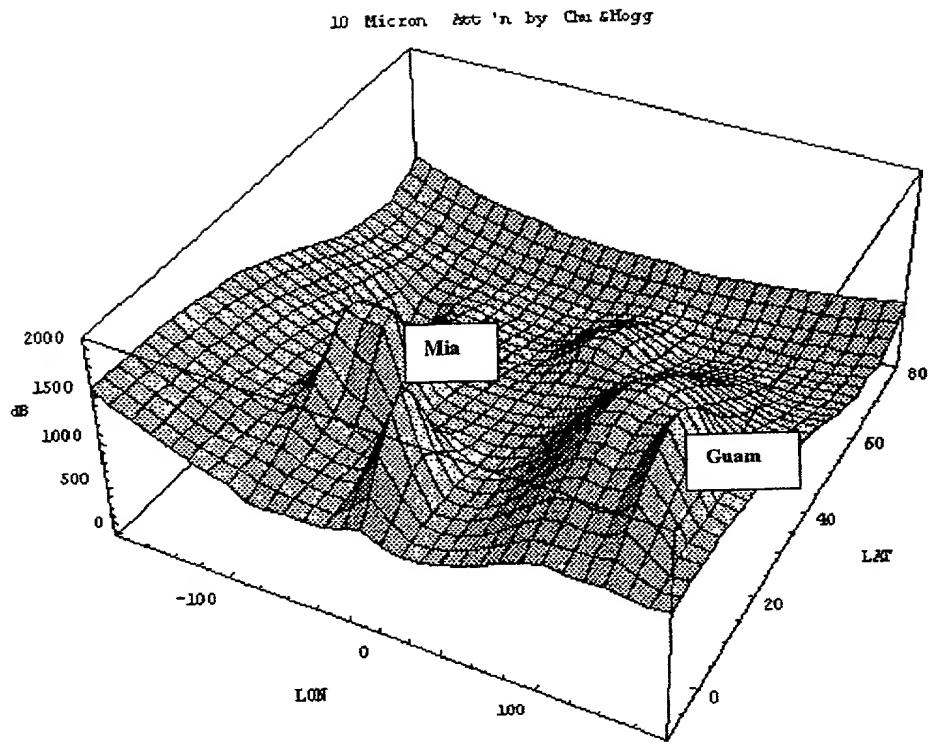


Fig. 2-9 Water Content of Clouds at 99% Non Rainy Condition from Barbaliscia and Chu&Hogg

The water mass approaches 3000 gm/m² in some parts of the tropics, as seen on Fig. 2-9. This would imply the very high infrared attenuation at zenith of Fig. 2-10.

The infrared attenuation at zenith of Fig. 2-10 is well beyond the comprehension of any useful communication system, and may indeed show why engineers have been frightened away from both infrared systems and optical systems. Zenith attenuation is shown to have zenith attenuation approaching 2000 dB in the tropics! It would certainly give justification to the JPL engineers who chose rare dry locations for the GOLD experiments. However, the infrared systems still have an ace up their sleeve: Barbaliscia also described attenuation in less difficult conditions (4) with 90%, 80%,-- ,50% non rainy availability levels. These conditions are much less imposing, and are treated in the next section.



**Fig. 2-10 10 Micron Cloud Attenuation by Barbaliscia, Chu&Hogg
99% Non Rainy Condition**

3.0 Reasonable Conditions for Infrared Communication

In their '97 paper Barbaliscia et al discussed probability distributions for attenuation throughout Europe and Northern Africa. We take the liberty to apply these distributions, which were nearly exponential, to similar attenuation regions around the world. The distributions are used for 10% exceedance levels and 20% exceedance levels, and will be seen to be considerably less severe than the 1% exceedance levels shown in the previous section. Fig. 3-1 shows cloud water content at 10% exceedance (90% non rainy availability).

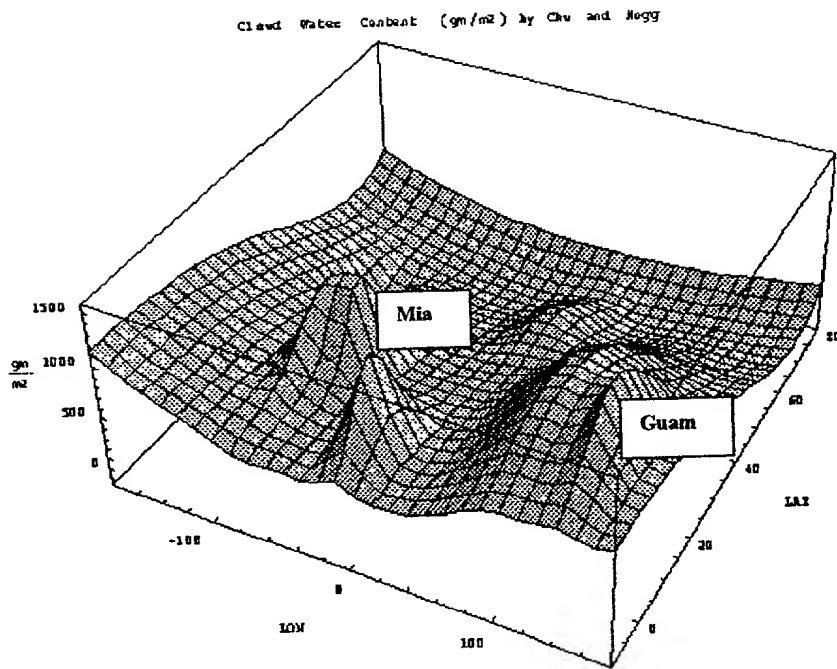


Fig. 3-1 Cloud Water Content at 10% Exceedance (90% non rainy)

Cloud water content is down sharply, for these 10% exceedance level cases, from the earlier 1% exceedance levels. 10 micron attenuation may be shown as Fig. 3-2.

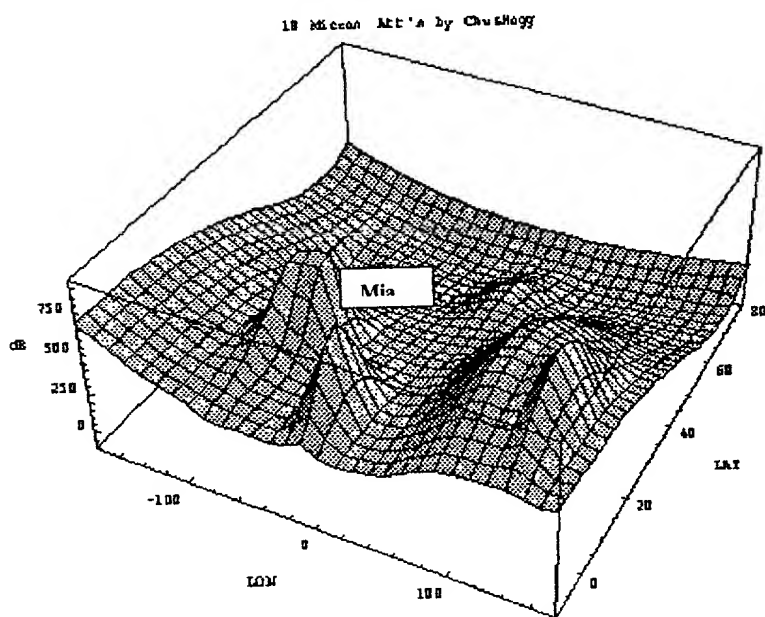


Fig. 3-2 10 Micron Attenuation at 10% Exceedance

Infrared communication would appear even more reasonable if 20% exceedance levels were allowable. At the conclusion, we will discuss a method for using the low cloud attenuation of the following figures. Figs. 3-3 and 4 indicate low water content and reasonable attenuation at 20% exceedance.

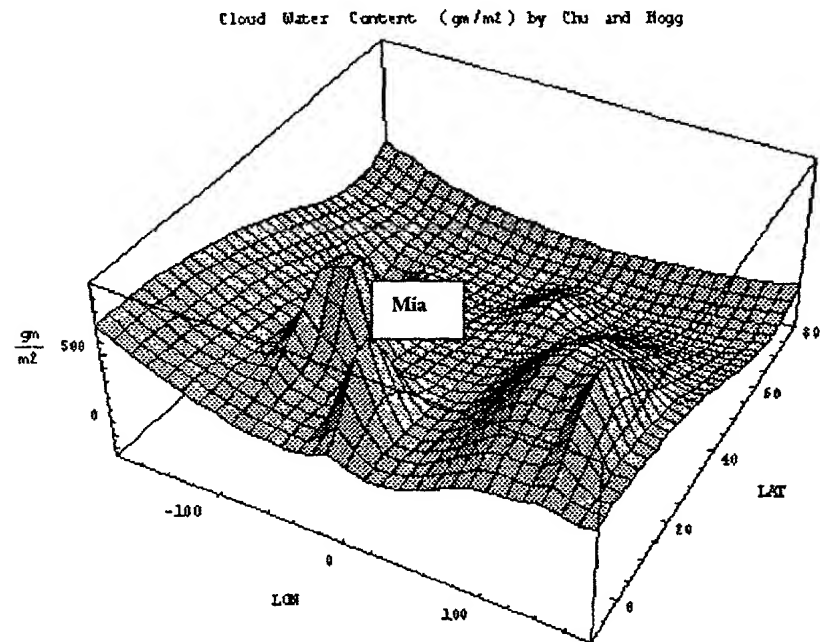


Fig. 3-3 Cloud Water Content at 20% Exceedance

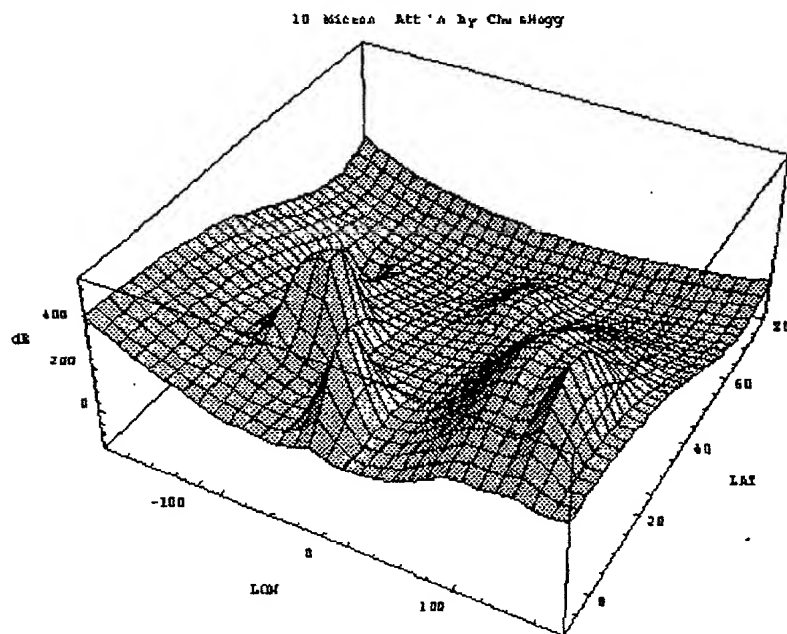


Fig. 3-4 10 Micron Attenuation at 20% Exceedance

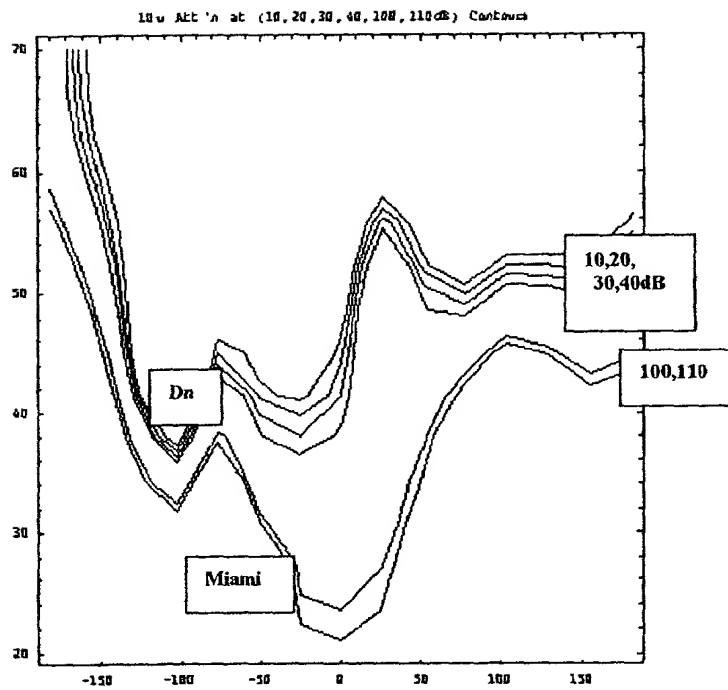


Fig. 3-5 10 Micron Attenuation Contours(dB) at 20% Exceedance; Denver(Dn)

The Temperate Zone attenuation contours of Fig. 3-5 indicate low zenith attenuation over large areas. Note large areas of the Rocky Mountains (40N, 100W) enjoy low attenuation, and the state of Maine might offer interesting infrared communication.

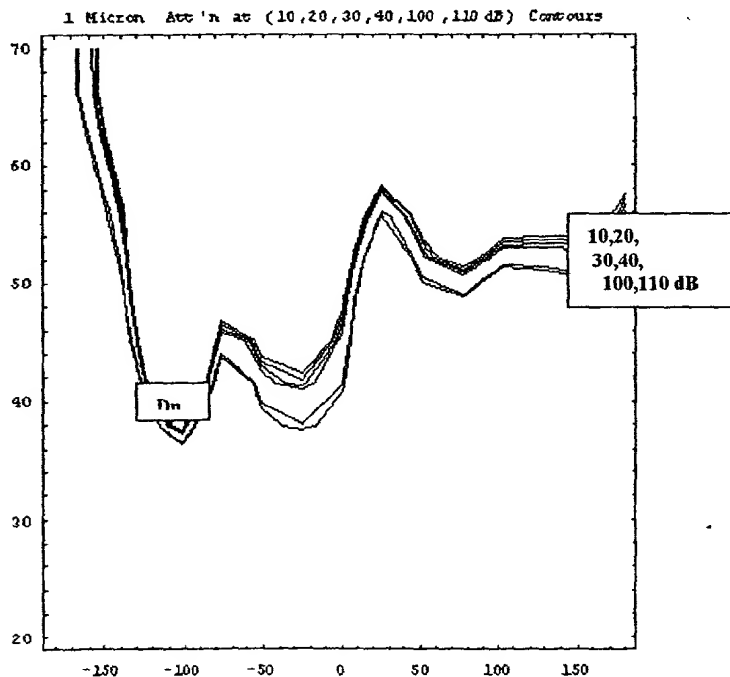
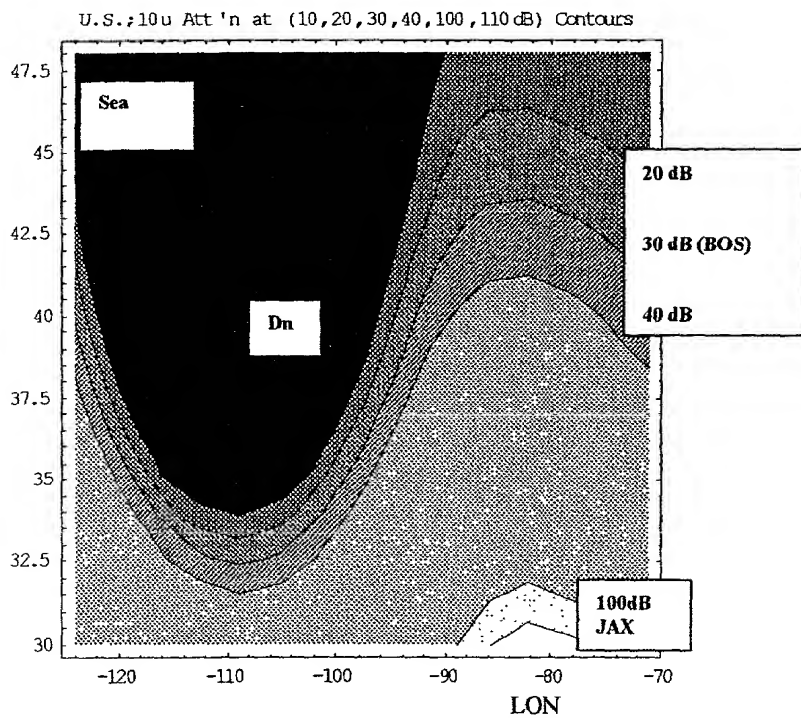


Fig. 3-6 One Micron Attenuation at 20% Exceedance

It is interesting to compare the useful communication areas on the East Coast of the U.S. at 10 microns and one micron. At 80 degrees west, the 40 dB attenuation contours occur at 40N for the 10 micron results (Fig. 3-5) and near 43N for one micron (Fig. 3-6). This suggests that the longer wavelength implies greatly expanded possibilities for communication on the East Coast.

4.0 A Closer Look at the United States

Zenith attenuation contours at 10 microns and 10% exceedance probability may be seen as Fig. 4-1, with 10,20,30, and 40 dB contours of most interest. As will be seen in the next section, the 20 dB contour offers an interesting performance comparison with millimeter wave systems. Note that Boston appears close to the 30 dB contour, but areas to the North (Maine) would be expected to offer attenuation at relatively modest attenuation. The attenuation approximation also appears to be too gross in the Northwest, where Seattle should be expected to have higher attenuation.



**Fig. 4-1 10 Micron Zenith Attenuation Contours for U.S.
80% Availability (20% Exceedance)
Seattle(Sea), Boston(BOS), Jacksonville(JAX), Denver(Dn)**

One micron attenuation contours are much higher, as seen on Fig. 4-2. The 100 dB contour is near Boston and the entire Northeast appears to offer difficult optical communication.

As we go to press, Hanson⁹ has shown new laser radar insights for a wide area of shipboard to aircraft conditions. The mid IR (three micron) region is favored over the nine micron region for high humidity, cloud free environments. Satellite communication should also have further comparisons between the three and 10 micron regions for humid ground sites.

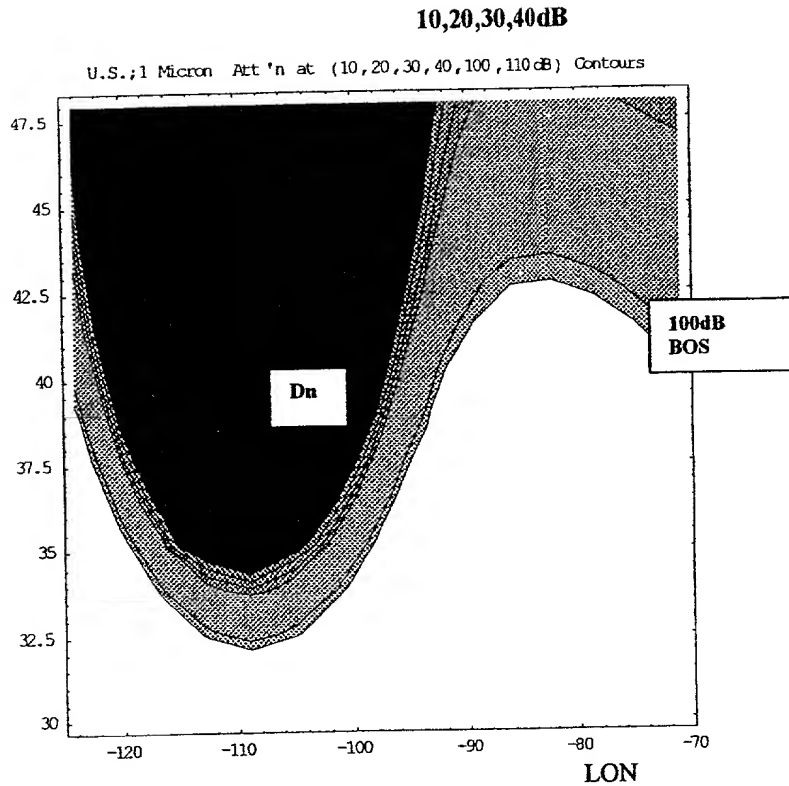


**Fig. 4-2 One Micron Zenith Attenuation Contours for U.S.
20% Exceedance Probability**

5.0 Interesting Wideband, Wide Area Communication

Laser communication typically has spectral availability more than 3 orders of magnitude greater than current wideband communication concepts at 30 GHz. This region is not only rich in frequency possibilities, it is also unhindered by government frequency regulations. Laser communication at one micron wavelength, with all its advantages, has the immense disadvantage for air- to- ground links of high cloud attenuation. This is why the GOLD experiment is restricted to a few unique sites.

Infrared communication at 10 microns will allow the ground sites to expand over large and interesting areas of the United States. Still, there would be availability concerns, with the attenuation maps of Sec. 3.0 showing low attenuation at 20% exceedance levels or only 80% availability. These concerns would be relieved by site diversity, with two separate sites on the order of 100 km apart for low ground site correlation as required by Soviet studies of cloud autocorrelation functions. Fiber optic lines could connect the two sites and switched diversity employed to choose the best signal. The availability of two sites would asymptotically approach 96% (or more! The Soviet studies also indicated *negative correlation* at certain distances). This availability is of the same order as that envisioned by Barbaliscia for many small millimeter wave satellite ground terminals. Quad diversity would approach conventional satellite availability requirements, with availability greater than 99.8%.

How much attenuation is reasonable for an infrared system that would be expected to compete with 30 GHz systems? Vincent Chan pointed out, in his 1985 intersatellite link studies, that 8 inch laser apertures should be expected to give similar performance as 8 foot millimeter wave apertures. This implies that, at constant small aperture, the laser system enjoys a 21 dB advantage in effective radiated power. The systems would be roughly equivalent in performance if the laser system suffered 21 dB loss. The 20 dB contour regions of the contour plots of Section 3.0 mark the bounds of the regions that indicate interesting performance comparisons with millimeter wave systems.

Why would a system designer be interested in the infrared region rather than the 30 GHz region? As international satellite expert Ed Ashford says, 'The 30 GHz region is the most oversubscribed region in history!' Current studies (7) show great promise for the 40 and 90 GHz regions, and perhaps an order of magnitude of spectrum might be achieved with expansion into those regions. This expansion might still cause an uneasy feeling because it would still leave the system designer deeply tied up with government frequency regulators, and systems may need more than an order of magnitude of new spectrum to fulfill internet needs within a few years. The infrared and optical regions may have a three order of magnitude spectral advantage over the 30 to 90 GHz range.

In conclusion we note that infrared communication systems would retain most of the outstanding advantages of optical systems, with small size, low cost, the ability to have all optical switching techniques with no required frequency changes, *plus* good communication capability over major areas of the U.S. (but clearly not all of the U.S.).

Objections to the 10 micron band have included the fact that solid state lasers have not been available in that band, but recent University of Vienna presentations at the September 2000 CLEO conference in Europe have shown consistently reliable solid state lasers at 11 microns. Also, recent Bell Labs announcements have heralded solid state developments at even longer wavelengths—up to 20 microns.

Finally, we reiterate the advantages of infrared systems over conventional 30 GHz concepts. The infrared systems would have orders of magnitude more spectral availability than the 30 GHz region, and would not require the systems designer to navigate through federal regulatory hoops. Of course, the 30 GHz systems would allow communication coverage of the entire U.S.

Support an Endangered Species

The millimeter wave attenuation maps have been invaluable in a variety of applications. If you appreciated them, this would be a good time to express your appreciation to:

F. Barbaliscia, Fondazione Ugo Bordoni, Viale Europa 190, 00144, Roma- Italy

Ph: +39 6 54802110, Fax: +39 6 54804401, Email: fbarba@fub.it

Selected References

1. K.E. Wilson *et al.*, "Overview of the Ground-to-Orbit Lasercom Demonstration," Free-Space Laser Comm. Tech IX, SPIE, Jan. 1997. The GOLD experiment was intended for ground to GEO communication with the Japanese ETS-VI satellite. Instead, the ETS-VI was stuck in the transfer orbit and only partial data was collected. The 1.024 MB/s links showed 10E-4 BER on the uplink and 10E-5 BER on the downlink.
2. I. Kim *et al.*, "(Very) Preliminary Results of the STRV-2 Satellite-to-ground Lasercom Experiment," Free-Space Laser Comm. Tech. XII, SPIE, vol. 3932, Jan. 2000.
3. T.S.Chi and D.C.Hogg, "Effects of Precipitation at 0.63, 3.5, and 10.6 Microns", Bell System Technical Journal, May-June 1968.
4. F. Barbaliscia, M. Boumis, A. Martellucci, "Characterization of Atmospheric Attenuation in the Absence of Rain in Europe in SHF/EHF Bands for VSAT Satcom Systems Applications," Ka Band Conference, Sorrento, Italy, Sept. 1997.
5. F. Barbaliscia, M. Boumis, A. Martellucci, "World Wide Maps of Non Rainy Attenuation for Low-Margin Satcom Systems Operating in SHF/EHF Bands," Ka Band Conference, Sept. 1998.
6. P. Christopher, "World Wide Millimeter Wave Attenuation Functions from Barbaliscia's 49/22 GHz Observations," Ka Band Conference, Taormina Sicily, Oct. 1999.
7. P. Christopher, "Satellite Constellations for Ka Band Communication," Ka Band Conference, Cleveland, Ohio, June 2000.
8. P. Christopher, editor, **Millimeter Wave Satellite Communication**, Vol. 1, Satellite Orbits, Vol.2 Propagation and Attractive Frequencies, PFC Associates, Leesburg, VA, May 2000. A few copies are available at: pfchristop@aol.com
9. Frank Hanson, "Coherent laser radar performance in littoral environments- a statistical analysis based on weather observations," Optical Engineering, Vol. 39 No. 11, Nov. 2000, 3044-3052.
10. Cloud water content equations are available on floppies (limited quantity) at pfchristop@aol.com

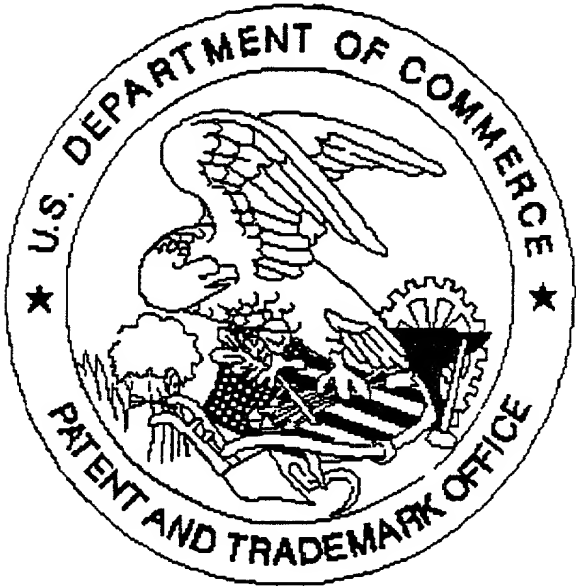
Appendix A Short Solution for Zenith Attenuation, as Function of Frequency(fg), LON,LAT

A longer, more accurate solution for millimeter wave attenuation is available on a floppy. Cloud water content maps are also available on a floppy¹⁰, loading under Mathematica.

LIEBE azen=

$$\begin{aligned}
 & 0.000408122 \text{ fg}^2 \left(5.34566 + 1.48098 E^{-\frac{1}{200}} (-10+\text{LAT})^2 - \frac{1}{200} (-145+\text{LON})^2 + 2.03295 E^{-\frac{1}{800}} (-18+\text{LAT})^2 - \frac{(-102+\text{LON})^2}{1800} + \right. \\
 & 1.1968 E^{-\frac{1}{200}} (-52+\text{LAT})^2 - \frac{1}{800} (-28+\text{LON})^2 - 2.78685 E^{-\frac{\text{LAT}^2}{1800}} - \frac{\text{LON}^2}{180000} + 2.48024 E^{-\frac{1}{72}} (-2+\text{LAT})^2 - \frac{1}{200} (7+\text{LON})^2 + \\
 & 1.41803 E^{-\frac{1}{50}} (-20+\text{LAT})^2 - \frac{1}{200} (60+\text{LON})^2 - 2.26449 E^{-\frac{1}{200}} (28+\text{LAT})^2 - \frac{1}{200} (77+\text{LON})^2 + \\
 & 1.69839 E^{-\frac{1}{200}} (-20+\text{LAT})^2 - \frac{1}{128} (82+\text{LON})^2 + 0.000898808 \text{ LAT} - 0.00187405 \text{ LAT}^2 + 8.15535 \times 10^{-7} \text{ LAT}^3 + \\
 & 1.92203 \times 10^{-7} \text{ LAT}^4 - 0.000690105 \text{ LON} - 5.83206 \times 10^{-6} \text{ LAT LON} + 3.42574 \times 10^{-7} \text{ LAT}^2 \text{ LON} + \\
 & 0.0000243378 \text{ LON}^2 + 1.15354 \times 10^{-8} \text{ LAT LON}^2 - 3.5046 \times 10^{-8} \text{ LON}^3 - 6.44437 \times 10^{-11} \text{ LON}^4 \left. \right) + \\
 & 0.00586939 \text{ fg}^2 \left(3.14686 + 0.665394 E^{-\frac{1}{200}} (-10+\text{LAT})^2 - \frac{1}{200} (-145+\text{LON})^2 + \right. \\
 & 1.1188 E^{-\frac{1}{800}} (-18,\text{LAT})^2 - \frac{(-102+\text{LON})^2}{1800} + 0.716478 E^{-\frac{1}{200}} (-52+\text{LAT})^2 - \frac{1}{800} (-28+\text{LON})^2 - \\
 & 1.18012 E^{-\frac{\text{LAT}^2}{1800}} - \frac{\text{LON}^2}{180000} + 1.21591 E^{-\frac{1}{72}} (-2+\text{LAT})^2 - \frac{1}{200} (7+\text{LON})^2 - 1.89544 E^{-\frac{1}{200}} (28+\text{LAT})^2 - \frac{1}{200} (77+\text{LON})^2 + \\
 & 0.8941 E^{-\frac{1}{200}} (-20+\text{LAT})^2 - \frac{1}{128} (82+\text{LON})^2 + 0.00101461 \text{ LAT} - 0.00094354 \text{ LAT}^2 + 2.75301 \times 10^{-7} \text{ LAT}^3 + \\
 & 1.00142 \times 10^{-7} \text{ LAT}^4 - 0.000268921 \text{ LON} - 1.63982 \times 10^{-6} \text{ LAT LON} + 2.33496 \times 10^{-7} \text{ LAT}^2 \text{ LON} + \\
 & 0.0000108872 \text{ LON}^2 + 1.02349 \times 10^{-8} \text{ LAT LON}^2 - 1.77808 \times 10^{-8} \text{ LON}^3 - 1.11299 \times 10^{-10} \text{ LON}^4 - \\
 & 0.201139 \left(5.34566 + 1.48098 E^{-\frac{1}{200}} (-10+\text{LAT})^2 - \frac{1}{200} (-145+\text{LON})^2 + 2.03295 E^{-\frac{1}{800}} (-18+\text{LAT})^2 - \frac{(-102+\text{LON})^2}{1800} + \right. \\
 & 1.1968 E^{-\frac{1}{200}} (-52+\text{LAT})^2 - \frac{1}{800} (-28+\text{LON})^2 - 2.78685 E^{-\frac{\text{LAT}^2}{1800}} - \frac{\text{LON}^2}{180000} + 2.48024 E^{-\frac{1}{72}} (-2+\text{LAT})^2 - \frac{1}{200} (7+\text{LON})^2 + \\
 & 1.41803 E^{-\frac{1}{50}} (-20+\text{LAT})^2 - \frac{1}{200} (60+\text{LON})^2 - 2.26449 E^{-\frac{1}{200}} (28+\text{LAT})^2 - \frac{1}{200} (77+\text{LON})^2 + \\
 & 1.69839 E^{-\frac{1}{200}} (-20+\text{LAT})^2 - \frac{1}{128} (82+\text{LON})^2 + 0.000898808 \text{ LAT} - 0.00187405 \text{ LAT}^2 + 8.15535 \times 10^{-7} \text{ LAT}^3 + \\
 & 1.92203 \times 10^{-7} \text{ LAT}^4 - 0.000690105 \text{ LON} - 5.83206 \times 10^{-6} \text{ LAT LON} + 3.42574 \times 10^{-7} \text{ LAT}^2 \text{ LON} + \\
 & 0.0000243378 \text{ LON}^2 + 1.15354 \times 10^{-8} \text{ LAT LON}^2 - 3.5046 \times 10^{-8} \text{ LON}^3 - 6.44437 \times 10^{-11} \text{ LON}^4 \left. \right) \\
 & \left(0.665418 - 132.118 (-0.740741 + 0.0333667 \text{ fg})^2 \right. \\
 & \left. \left(0.999375 - 11.4943 \sqrt{(-0.740741 + 0.0333667 \text{ fg})^2} \text{ ArcTan} \left[\frac{0.0869456}{\sqrt{(-0.740741 + 0.0333667 \text{ fg})^2}} \right] \right) - \\
 & 132.118 (0.740741 + 0.0333667 \text{ fg})^2 \\
 & \left. \left(0.999375 - 11.4943 \sqrt{(0.740741 + 0.0333667 \text{ fg})^2} \text{ ArcTan} \left[\frac{0.0869456}{\sqrt{(0.740741 + 0.0333667 \text{ fg})^2}} \right] \right) - \right. \\
 & 0.00392386 \text{ fg}^2 \left(18.2482 \left(\text{Log} \left[\frac{(2 - 0.0333667 \text{ fg})^2}{0.000749822 + (2 - 0.0333667 \text{ fg})^2} \right] + \right. \right. \\
 & \text{Log} \left[\frac{(3.959999999999999 - 0.0333667 \text{ fg})^2}{0.000187456 + (3.959999999999999 - 0.0333667 \text{ fg})^2} \right] + \\
 & \text{Log} \left[\frac{\left(\frac{61}{10} - 0.0333667 \text{ fg} \right)^2}{0.000187456 + \left(\frac{61}{10} - 0.0333667 \text{ fg} \right)^2} \right] + \text{Log} \left[\frac{(2 + 0.0333667 \text{ fg})^2}{0.000749822 + (2 + 0.0333667 \text{ fg})^2} \right] + \\
 & \text{Log} \left[\frac{(3.959999999999999 + 0.0333667 \text{ fg})^2}{0.000187456 + (3.959999999999999 + 0.0333667 \text{ fg})^2} \right] + \\
 & \text{Log} \left[\frac{\left(\frac{61}{10} + 0.0333667 \text{ fg} \right)^2}{0.000187456 + \left(\frac{61}{10} + 0.0333667 \text{ fg} \right)^2} \right] + \\
 & 27.7778 \text{ Log} \left[\frac{0.00111334 \text{ fg}^2}{0.000323595 + 0.00111334 \text{ fg}^2} \right] \left. \right)
 \end{aligned}$$

United States Patent & Trademark Office
Office of Initial Patent Examination -- Scanning Division



Application deficiencies found during scanning:

Page(s) _____ of _____ were not present
for scanning. (Document title)

Page(s) _____ of _____ were not present
for scanning. (Document title)

Scanned copy is best available. Drawings are all fig dark